Turn-on time delay characteristics of external cavity laser based polymer fiber gratings

HISHAM K. HISHAM[1,*], AHMAD F. ABAS[2], MOHD A. MAHDI[3]
[1]*Department of Electrical Engineering, College of Engineering, Basra University, Basra 61001, Iraq*
[2]*Department of Electrical Engineering, College of Engineering, King Saud University, Riyadh 11421, Saudi Arabia*
[3]*Department of Computer and Communication Systems Engineering, Faculty of Engineering, Universiti Putra Malaysia, 43400 Serdang, Malaysia*

The turn-on time delay (T_{Delay}) characteristics of an external cavity laser-based polymer fiber gratings (PFGs) is successfully investigated. Numerical optimization of model parameters is used to reduce the laser T_{Delay} by analyzing the effects of the laser injection current (I_{inj}), the temperature (T) variation, the recombination rate $R(N)$ coefficients, and the external OFB level on T_{Delay}. Results show that the effect of $R(N)$ coefficients are to increase the T_{Delay} value and not decrease it as written in the previous studies. Also, results show that the T_{Delay} value is increased when T is increased. However, we can eliminate it either by increasing the ρ value (i.e. $\rho = N_i/N_{th}$) at a fixed value of I_{inj} or by increasing the σ value (i.e. $I_{inj} = \sigma \times I_{th}$) at constant I_{th}. In addition, we can use the external optical feedback (EOF) level as a controller for reducing the T_{Delay} value or to turn-on the laser by controlling the N_{th} value depending on the EOF level.

(Received June 9, 2022; accepted November 24, 2023)

Keywords: External cavity laser, Optical fiber, Polymer Bragg grating, Semiconductor laser, Dynamic response

1. Introduction

The last two decades of the last century, due to the growing demand for massive data transmission, showed a noticeable increase in the use of optical fiber gratings (FGs) as an indispensable tool in many important applications [1-4], where the external environment such as stress [5, 6] and temperature [7- 9] plays a dominant role due to its unique characteristics such as wavelength selection [10-12] and low loss [13-15]. However, for silica fiber gratings (SFGs), limited tunability is a major drawback of this important tool [3, 4] which reduces its reliability in many important applications [13-15].

In the case of polymer fiber gratings (PFGs) the situation is totally different; the thermal and strain characteristics are much higher than that of the SFGs [16]. For example, the Young's modulus for the polymer is 70 times smaller than that of silica (i.e. 0.1 x 10^{10} N/m^2 compare with 7.13 x 10^{10} N/m^2), which make the mechanical tunability is much better than that of SFGs. In addition, PFGs has the merits of a large thermo-optic effect, thereby, large refractive index tuning can be obtained. Furthermore, the flexibility of the PFGs can make the tunability extend beyond the thermo-optic effect limit [17]. Based on the mention facts, PFGs has better potential to be used as wavelength tuning and sensing element.

The widespread use of systems based on wavelength division multiplexing (WDM) networks [18-20], which are characterized by their complete reliance on a highly stable laser source with a large possibility of tuning, make fiber gratings (FGs) based on external cavity lasers (ECLs) an indispensable source [21-24]. The reason for this is that the ECL emission wavelength depends only on the Bragg wavelength of the FGs and does not depend on the injection current (Iinj) of the laser cavity [25-27]. Therefore, ECLs are a promising source of light for receiver-dense WDM (DWDM) systems. Furthermore, the wavelength of FGs can be controlled more precisely than other laser models. As a result, ECLs achieve much better wavelength control [28, 29].

Generally, in laser diodes (LDs), a parameter known as a turn on time delay (T_{Delay}) is very important. It is defined as the time required for populating the carriers (N) to reach its threshold level (N_{th}) where the initial level of current (I_o) changes to any current value (I) larger than its laser threshold current (I_{th}). This happens when LDs are injected by an injection current (I_{inj}) [30]. During this period, the concentration of photons (P) suffers a relaxation oscillation until it reaches its steady state value [31]. For longer T_{Delay} value, the relaxation oscillation period is also longer, which may result a significant error in received-data when the laser is used in high-speed transmission systems [30 -31].

The T_{Delay} is one of the most important parameters that play a major role in determining the performance characteristics of the communication systems [31]. It was found that it is strongly dependent on the functional form of the carrier recombination rate $R(N)$ coefficients [30-32]. However, most of the previous studies relied in their results on approximate relationships or equations in which one or more of the influential parameters were neglected [30, 33]. In addition to the inaccuracy in the results, these assumptions cancel out the influence of some important parameters in determining the true dynamic behavior of the system. On the other hand, to our knowledge there is no study that dealt with this important parameter of ECLs based on PFGs, as all previous studies were concerned with SFGs.

The continuous increase in the versatility of promising applications within the optical communication systems and optical sensing fields makes PFGs an indispensable tool in the coming days, so studying the dynamic properties of PFGs based on ECLs is essential.

2. Laser model

A schematic diagram of the ECL model is shown in Fig. 1. In this model, ECL consists of Fabry-Perot (FP) laser diode with length L_d .The front facet reflectivity is approximately zero ($R_1 \approx 0$), while the rear facet has a finite reflectivity R_o that is coupled to a single-mode fiber (SMF) of length L_f with coupling coefficient C_o. The PFGs with reflectivity r_{FBG} is connected at the end of SMF.

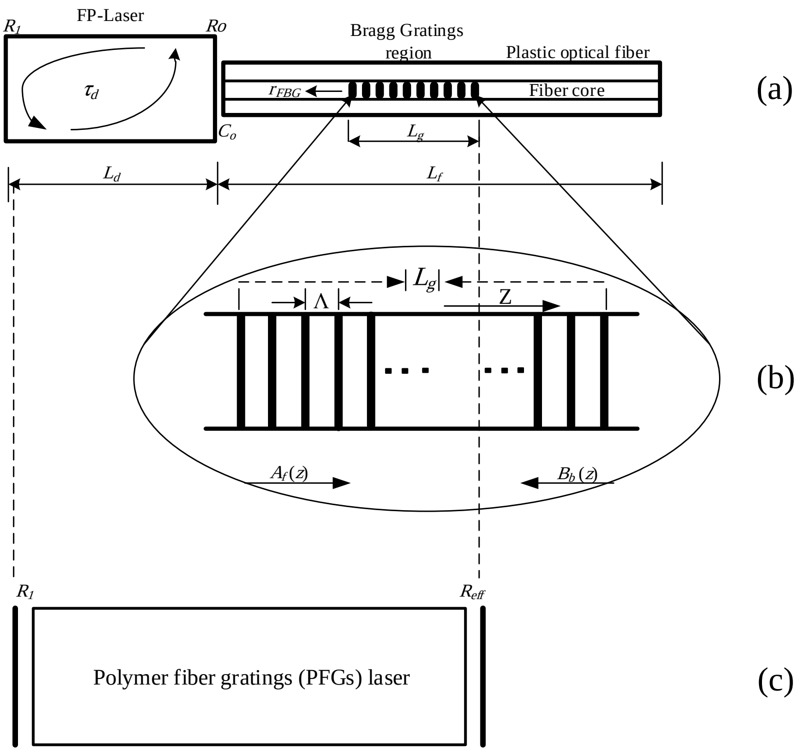

Fig. 1. ECL model based PFGs

Based on Fig. 1 (c), the effective reflectivity R_{eff} is given by [32]

$$R_{eff} = \left|r_{eff}\right|^2 = \left|R_o\left(1 + F_{ext} \times \cos(2\pi v \tau_e)\right)\right|^2 \quad (1)$$

where v is the optical frequency, $\tau_e = 2n_{ext}L_f / c$ is the round-trip delay of photons inside the external cavity, $c = 3\times10^{10}$ cm/s is the velocity of light in vacuum, n_{ext} is the external cavity refraction index and F_{ext} is a factor is due to the external cavity given by [32]

$$F_{ext} = \frac{r_{ext}}{R_o}\left(1 - \left|R_o\right|^2\right) \quad (2)$$

where r_{ext} is the external optical feedback (EOF) reflection coefficient of the PFGs.

By considering the combine effect of the temperature (T) and external optical feedback (EOF), the threshold current [9] is given as

$$I_{th,\mathrm{EOF}}(T) = eVN_{th,\mathrm{EOF}}(T)R(T, N_{th,\mathrm{EOF}}) \quad (3)$$

In Eq. (3), e is the electronic charge, V is the active region volume and $R(T, N_{th,EOF})$ is the carriers recombination rate [31] can be rewritten as

$$R(T, N_{th,EOF}) = A_{nr} + BN_{th,EOF}(T) + CN_{th,EOF}^2(T) \quad (4)$$

where, A_{nr} is the nonradiative recombination rate, B is the radiative recombination rate and C is the Anger recombination rate, respectively. In Eq. (4), the

$N_{th,\mathrm{EOF}}(T)$ represent the threshold carrier density [31], can be defined as

$$N_{th,\mathrm{EOF}}(T) = N_t(T) + \frac{1}{\Gamma v_g g(T)\tau_{p,\mathrm{EOF}}(T)} \quad (5)$$

In Eq. (5), $N_t(T)$ represent the carrier density at transparency, $g(T)$ is the gain coefficient, and $\tau_{p,\mathrm{EOF}}(T)$ is the photon life time which can be modeled as [31]

$$\tau_{p,\mathrm{EOF}}(T) = \frac{1}{v_g \alpha_{tot,\mathrm{EOF}}(T)} \quad (6)$$

where $\alpha_{tot,\mathrm{EOF}}(T)$ is the total cavity loss that is defined as [31]

$$\alpha_{tot,\mathrm{EOF}}(T) = \alpha_{\mathrm{int}}(T) + \frac{1}{2L_d}\ln\left(\frac{1}{R_1 R_{eff}}\right) \quad (7)$$

In Eq. (7), $\alpha_{\mathrm{int}}(T)$ and $\left((1/2L_d)\ln\left(1/R_1 R_{eff}\right)\right)$ represents the internal cavity and the mirror losses, respectively. According to the Eqs. (1) – (7), the $N_{th,\mathrm{EOF}}(T)$ can be expressed as

$$N_{th,\mathrm{EOF}}(T) = N_t(T) + \Theta(T) \quad (8)$$

where,

$$\Phi(\mathrm{T}) = \frac{\left(\alpha_{\mathrm{int}}(T) + \frac{1}{2L_d}\ln\frac{1}{R_1\left|R_2\left(1+F_{ext}\times\cos(2\pi\nu\tau_e)\right)\right|^2}\right)}{\Gamma g(T)} \quad (9)$$

Equation (8) represent the expression for the carrier density under the threshold condition of the ECL model.

3. The T_{Delay} formula of ECL model based PFGs

As we have defined in the introduction part, the T_{Delay} represent the time is needed by the carrier density (N) to increases from a specified initial value (N_i) to the threshold one (N_{th}). This time (i.e. T_{Delay}) can be calculated by [31]

$$T_{Delay} = \int_{N_i}^{N_{th,EOF}} \frac{eV}{I_{inj} - eVN(A_{nr} + BN + CN^2)}dN \quad (10)$$

After considering the effect of the R_{eff} for the PFGs given in Ref. [31], Eq. (10) can be solved numerically to study the T_{Delay} characteristics of the ECL model based PFGs. This solution can be written as [31]

$$T_{Delay} = \xi\Pi_1 \mathrm{X1} + \xi\Pi_2 \mathrm{X2} + \xi\Pi_3 \mathrm{X3} \quad (11)$$

where,

$$\mathrm{X1} = \ln\left[\frac{\Theta\left(\Pi_1, N_{th,\mathrm{EOF}}\right)}{\Theta\left(\Pi_1, \rho N_{th,EOF}\right)}\right] \quad (12)$$

$$\mathrm{X2} = \ln\left[\frac{\Theta\left(\Pi_2, N_{th,\mathrm{EOF}}\right)}{\Theta\left(\Pi_2, \rho N_{th,\mathrm{EOF}}\right)}\right] \quad (13)$$

$$\mathrm{X3} = \ln\left[\frac{\Theta\left(\Pi_3, N_{th,\mathrm{EOF}}\right)}{\Theta\left(\Pi_3, \rho N_{th,EOF}\right)}\right] \quad (14)$$

$$\Theta(\Pi_m, N) = B + \Xi 1\Pi_m + \Xi 2N \quad (15)$$

$$\Xi 1 = \left(A_{nr}B\xi + 9CI_{inj}\right) \quad (16)$$

$$\Xi 2 = \left[\left(2B^2 - 6A_{nr}C\right)\xi\Pi_m + 3C\right] \quad (17)$$

$$\Pi_1 = \frac{1}{6\xi}\frac{\Re_2}{\Re_1} + 2\left(3A_{nr}C - B^2\right)\frac{\xi}{\Re_4} \quad (18)$$

$$\Pi_2 = \frac{-1}{2}\Phi 1 + j\frac{\sqrt{3}}{2}\Phi 1 \quad (19)$$

$$\Pi_3 = \frac{-1}{2}\Phi 1 - j\frac{\sqrt{3}}{2}\Phi 1 \quad (20)$$

$$\Phi 1 = \left(\frac{1}{6\xi}\frac{\Re_2}{\Re_1} + 2\left(3A_{nr}C - B^2\right)\frac{\xi}{\Re_4}\right) \quad (21)$$

$$\Re_1 = \xi^2 A_{nr}^2\Omega 1 + \xi BI_{inj}\Omega 2 + 27C^2 I_{inj}^2 \quad (22)$$

$$\Omega 1 = \left(4A_{nr}C - B^2\right) \quad (23)$$

$$\Omega 2 = \left(18A_{nr}C - 4B^2\right) \quad (24)$$

$$\Re_2 = \left[\xi^2\Re_1\left(-108C + 12\sqrt{3}\Re_3^{1/2}\right)\right]^{1/3} \quad (25)$$

$$\Re_3 = \frac{\Re_4}{\Re_1} \quad (26)$$

$$\Re_4 = 4\xi^2 B^2 \Omega 3 + 108\xi B C^2 I_{inj} \Omega 4 + 729 C^4 I_{inj}^2 \quad (27)$$

$$\Omega 3 = \left(20.25 A_{nr}^2 C^2 - 9 A_{nr} B^2 C + B^4\right) \quad (28)$$

$$\Omega 4 = \left(4.5 A_{nr} C - B^2\right) \quad (29)$$

Also, $\xi = eV$ and ρ $(0\langle\rho\langle 1)$ represents the ratio of the N_i to the (i.e. $\rho = N_i / N_{th}$).

4. Results and discussion

In our numerical analysis, constant value of injection current is assumed; $I_{inj} = \sigma \times I_{th}$ (σ is an integer value) and it is independent of I_{th}. For other main parameters, the common values used in the analysis are tabulated in Table 1.

Table 1. Parameters of ECL model based PFGs at room temperature (25ºC)

Parameter	Description
$L_d = 400\mu m$	Cavity length
$d = 0.1\mu m$	Active region thickness
$w = 2\mu m$	Active region width
$N_o = 1.10^{24} m^{-3}$	Transparency carrier density
$A_{nr} = 1.10^8 \sec^{-1}$	Nonradiative recombination coefficient
$B = 1.10^{-16} m^3/\sec$	Radiative recombination coefficient
$C = 3.10^{-41} m^6/\sec$	Auger recombination coefficient
$\alpha_{int} = 1000 m^{-1}$	Internal cavity loss
$\Gamma = 0.34$	Field confinement factor
$a_o = 2.5.10^{-20} m^2$	Differential gain
$L_{FBG} = 4mm$	Grating length
$\lambda = 1550$ nm	Operating wavelength

Fig. 2 shows T_{Delay} for PFGs model as a function to the carrier density ratio (i.e. $\rho = N_i / N_{th}$) for different values of σ at reference temperature ($T = 25^o C$).

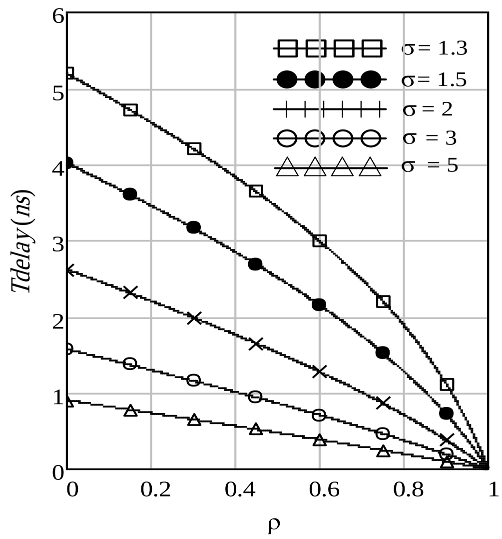

Fig. 2. Turn-on delay time function to ρ for different values of σ

As shown, with the increases of the ρ value, T_{Delay} reduces. This result agrees with the assumption that, when N_i reaches N_{th}, the T_{Delay} value will be zero [31]. As a result, when the laser biased near N_{th}, the T_{Delay} can be eliminated.

Fig. 3 shows a comparison between the T_{Delay} calculation by our exact numerical expression model and other approximated equations in the previous studied [30, 31, 33] for $\sigma = 1.3$. As shown, there are differences in the T_{Delay} values. This difference is due to the neglected one or more of the $R(N)$ coefficients (i.e. A_{nr}, B, C). The validity of our results can be confirmed by the following interpretation: according to Eq. (4), any increment in the A_{nr}, B, and C; the T_{Delay} increases due to the increases of the carrier recombination rate time; $R(N)$ which results in an increase in the threshold current of the laser (i.e. Eq. (3)).

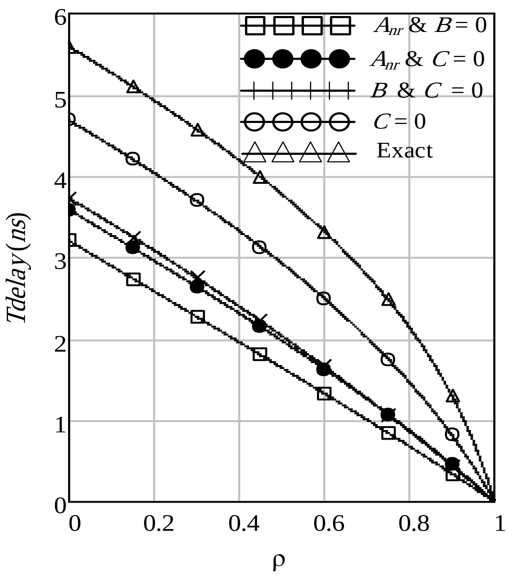

Fig. 3. A comparison among various expressions of turn-on delay time with ρ at σ = 1.3

As it is known, the higher the threshold current (I_{th}), the greater T_{Delay} required to reach the threshold value. This meaning that, the effect of increasing any one of the *R(N)* coefficients, is to increase the T_{Delay} value as shown in Fig. 4. It is important to mention here that this result is completely contrary to that is given in the [33]. Thus, according to the results given in Fig. 4, the general effect of the $R(N)$ coefficients are to increases the T_{Delay} value as they increase. So the T_{Delay} can be reduce either by reduce $R(N)$ coefficients at fixed value for I_{inj} or by increasing I_{inj} at constant I_{th}. These results indicate preference model proposed by us compared with previous studies.

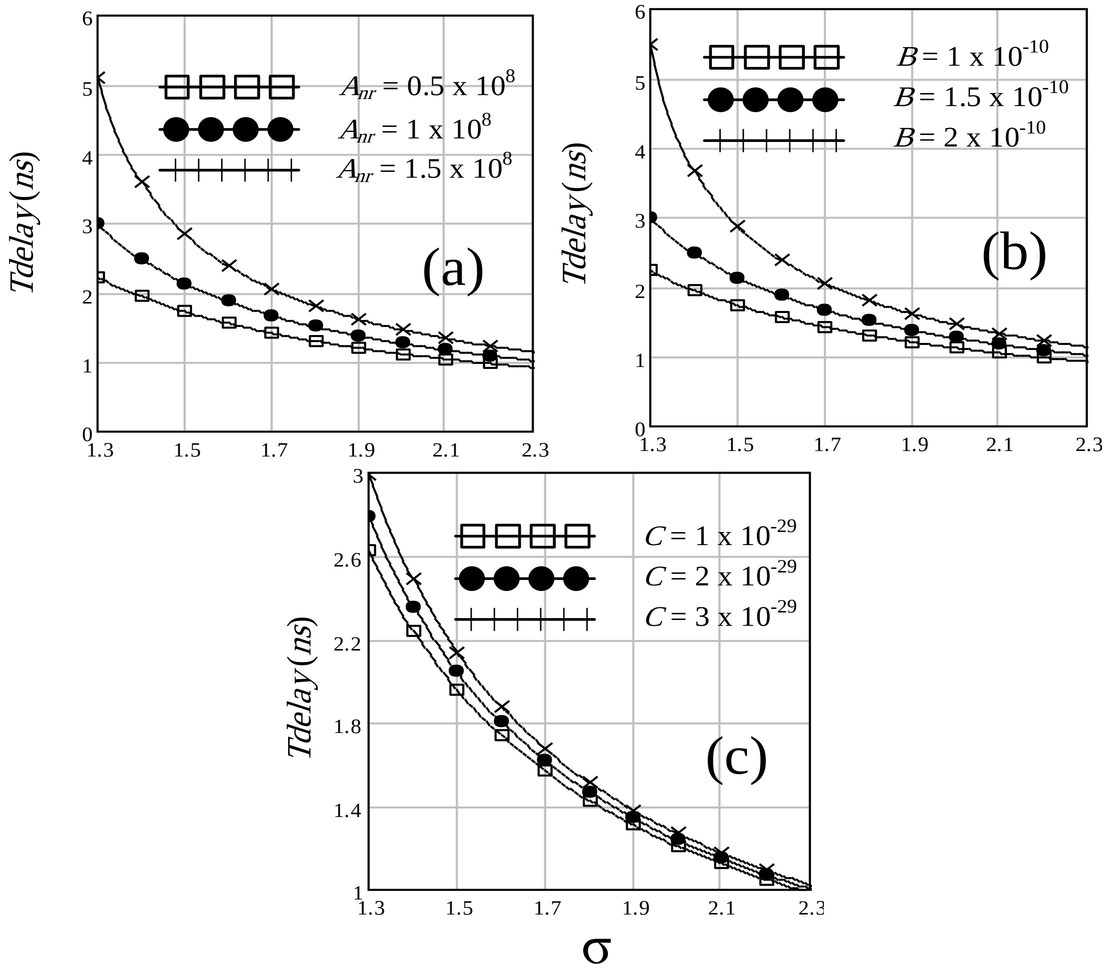

Fig. 4. Effect of R(N) coefficients on turn-on time delay at ρ = 0.5. (a) A_{nr}, (b) B and (c) C coefficients, respectively

Fig. 5 (a) and (b) shows the effect of temperature (T) on T_{Delay} for different values of ρ at $\sigma = 1.3$ for PFGs and SFGs, respectively. In general, it is clear that the T_{Delay} is increases with the increase of T due to its effect on the N_{th} value (i.e. according to Eq. (8)). However, the effect of temperature can be eliminated by increasing of the ρ value. This result can explain as, when $\rho \to 1$, i.e. $N_i \to N_{th}$, therefore, $T_{Delay} \to 0$. Thus, when the laser source turned on from N_i closed to the N_{th} value, the T_{Delay} can be eliminate. Also according to the results shown in Fig. 5, the ρ value is represented a significant factor for reducing the T_{Delay} value especially in the direct modulation of LDs where N_i is varied depending on the time intervals. Thus, if the time interval is relatively short, then, the value of ρ have the significant effect in reducing T_{Delay}.

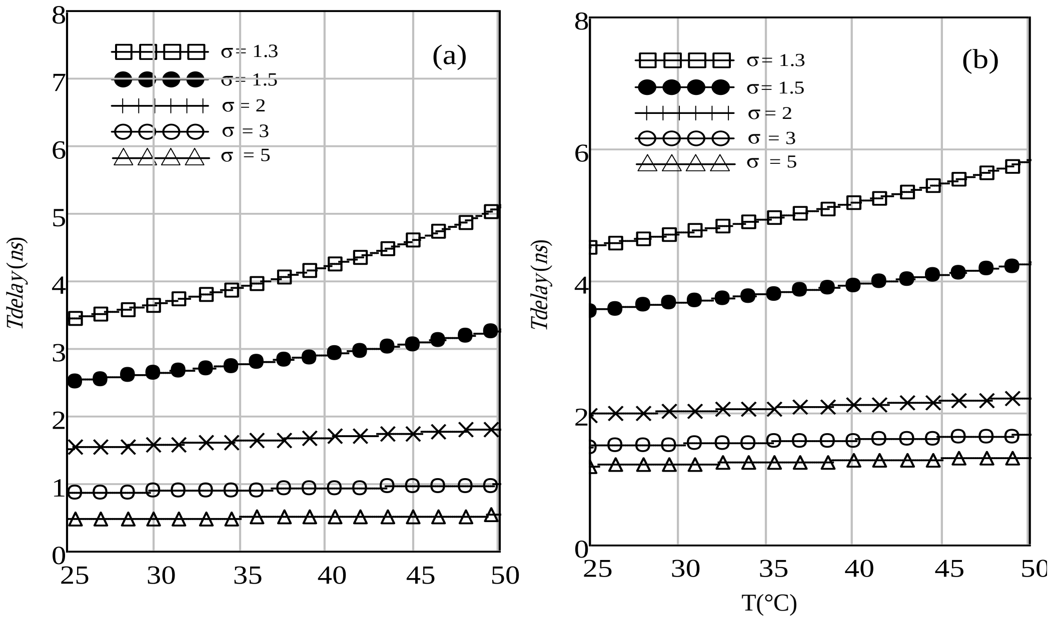

Fig. 5. Effect of temperature on T_{Delay} for different values of σ at ρ = 0.5. (a) PFGs and (b) SFGs

On the other hand, by comparing Fig. 5 (a) and (b), it can be seen that there is a difference between the T_{Delay} value for the two cases. And to be more precise, the T_{Delay} in the case of the PFGs with the change in temperature is less than it is in the case of SFGs. The reason for this is due to the change of the R_{eff} value of both cases with temperature as shown in Fig. 6 which in turn greatly affects the T_{Delay} value based on the Eqs. (1) - (29). Also, the results in Fig. 5 show that with the increase of the σ value, the T_{Delay} is reduced at specified value of ρ and the effect of temperature is eliminated. Thus, depending on the results shown in Fig. (5), the effect of temperature on T_{Delay} can be eliminate either by increasing of the ρ value at a fixed injection current (I_{inj}) or by increasing of the σ value at constant I_{th}.

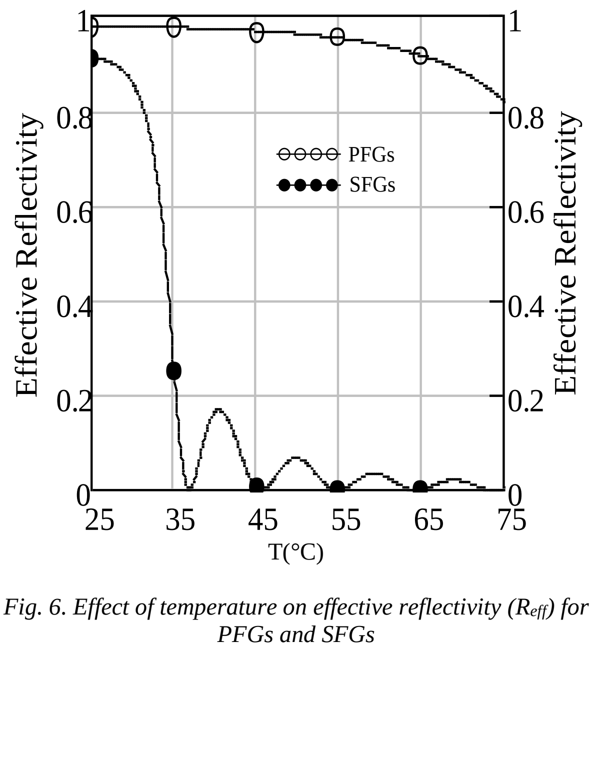

Fig. 6. Effect of temperature on effective reflectivity (R_{eff}) for PFGs and SFGs

Finally the effect of external optical feedback (EOF) reflectivity; R_{ext} on the T_{Delay} as a function of σ at $\rho = 0.5$ is shown in Fig. 7. As shown, the T_{Delay} value is decreases with the increase of the R_{ext} value. The reason for this can be explained as follows: by increasing the R_{ext} value, the R_{eff} will increase (i.e. Eq. (1)) and that results in a reduction in the total cavity loss (i.e. Eq. (7)), and an increasing in the photon life time (i.e. Eq. (6)). Consequently, the N_{th} value will decrease as given in Eq. (8). This result suggests that EOF can be used as a controller or an optical switching circuit to laser turn-on by controlling the N_{th} value.

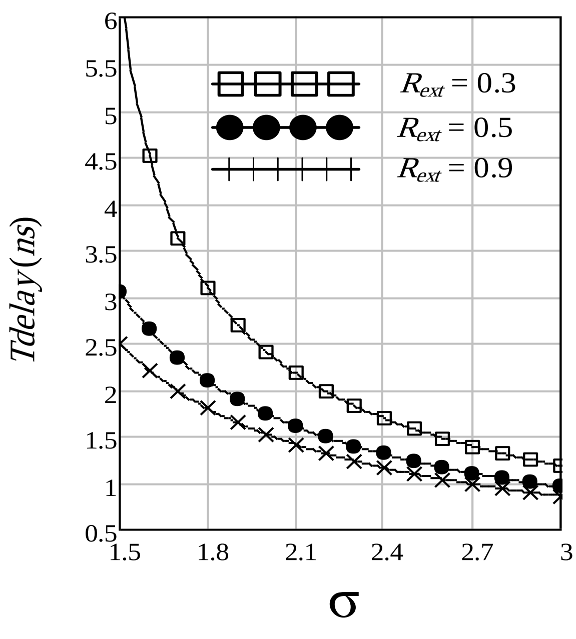

Fig. 7. Effect of R_{ext} on turn-on time delay at ρ = 0.5

5. Conclusion

A numerical study on the turn-on time delay (T_{Delay}) characteristics of an external cavity laser (ECL) model-based polymer fiber gratings (PFGs) is successfully investigated. The analysis has done based on an exact numerical formula and not by using approximated formulas as in previous studies. Results show that the effect of the $R(N)$ coefficients is to increasing the T_{Delay} value and not as reported in the previous studies. Also, results show that, the effect of temperature is to increase the T_{Delay} and it is effect is less than that of the SFGs. However, temperature effect can be eliminated either by increasing ρ at a fixed value of injection current (I_{inj}) or by increasing σ at constant laser threshold current (I_{th}). In addition, we can put down or reducing the T_{Delay} value by controlling the N_{th} value through the use of the EOF level.

References

[1] B. Jiang, J. Zhao, J. Lightwave Technol. **41**, 4103 (2023).
[2] X. Gui, Zhengying Li, Xuelei Fu, Huiyong Guo, Yiming Wang, Changjia Wang, Jiaqi Wang, Desheng Jiang, J. Lightwave Technol. **41**, 4187 (2023).
[3] V. Reimer, A. Abdalwareth, G. Flachenecker, U. Willer, M. Angelmahr, W. Schade, J. Lightwave Technol. **41**, 4366 (2023).
[4] G. M. Berruti, P. Vaiano, A. Boniello, S. Principe, G. Quero, G. V. Persiano, M. Consales, A. Cusano, J. Lightwave Technol. **40**, 797 (2022).
[5] T. Tan, Y. Xie, C. Duan, Q. Chai, Y. Chu, G. Sun, Y. Luo, Y. Tian, J. Zhang, IEEE Transactions on Instrumentation and Measurement **71**, 1(2022).
[6] J. Zhang, T. Tan, C. Duan, Z. Li, X. Liu, Q. Chai, G. Xiao, Y. Tian, W. Zhang, Y. Xu, IEEE Transactions on Instrumentation and Measurement **71**, 1(2022).
[7] Q. Bian, F. J. Dutz, M. Lindner, F. Buchfellner, A. Stadler, M. Jakobi, A. W. Koch, J. Roths, J. Lightwave Technol. **41**, 3175 (2023).
[8] Y.-L. Wang, Y. Tu, S. -T. Tu, IEEE Sensors J. **21**, 4652 (2021).
[9] Y. Zhao, S. Liu, J. Luo, Y. Chen, C. Fu, C. Xiong, Y. Wang, S. Jing, Z. Bai, C. Liao, Y. Wang, J. Lightwave Technol. **38**, 2504 (2020).
[10] S. Chen, Y. Zhao, M. Tang, Z. Hua, H. Peng, Y. Ma, Y. Liu, Asia Communications and Photonics Conference (ACP), Shenzhen, China, 218 (2002).
[11] Z. Liu, X. Zhao, C. Mou, Y. Liu, J. Lightwave Technol. **38**, 1536 (2020).
[12] N. Deng, L. Zong, H. Jiang, Y. Duan, K. Zhang, J. Lightwave Technol. **40**, 3385 (2022).
[13] G. Rajan, B. Liu, Y. Luo, E. Ambikairajah, G.-D. Peng, IEEE Sensors J. **13**, 1794.
[14] L. Leffers, J. Locmelis, K. Bremer, B. Roth, L. Overmeyer, IEEE Photon. J., **13**, 1 (2021).
[15] Y. Zhang, D. Feng, Z. Liu, Z. Guo, X. Dong, K. S. Chiang, B. C. B. Chu, IEEE Photonics Technology Letters **13**, 618 (2001).
[16] A. G. Leal-Junior, A. Frizera, C. Marques, IEEE Photonics Technology Letters **32**, 623 (2020).
[17] H. Hisham, Iraqi J. Elect. Electron. Eng. **12**, 85 (2016).
[18] C. W. Chow, J. Y. Sung, C. H. Yeh, IEEE Photonics J. **7**, 1 (2015).
[19] J. M. Buset, Z. A. El-Sahn, D. V. Plant, IEEE Photonics Technol. Lett., **25**, 1435 (2013).
[20] C.-H. Yeh, C.-W. Chow, C.-H. Hsu, IEEE Photonics Technology Letters **22**, 118 (2010).
[21] J. H. Lee, M. Y. Park, C. Y. Kim, C. Seung-Hyun, W. Lee, G. Jeong, B. W. Kim, I IEEE Photonics Technology Letters **17**, 1956 (2005).
[22] G. Jeong, J.-H. Lee, M.Y. Park, C.Y. Kim, S.-H. Cho, W. Lee, B.W. Kim, IEEE Photonics Technology Letters **18**, 2102. (2006).
[23] S. H. Oh, Y. Ki-Hong, K. So Kim, J. Kim, O. Kyun Kwon, D. Kon Oh, Y. Noh, S. Jun-Kyn, L. Hyung-Jong, IEEE J. Selected Topics in Quantum Electron. **17**, (2011).
[24] K.-J. Kim, M.-C. Oh, S.-R. Moon, C.-H. Lee, J. Lightwave Technol. **31**, 982 (2013).
[25] L. Zhang, F. Wei, G. Sun, D.-J. Chen, H.-W. Cai, R.-H. Qu, IEEE Photonics Technology Letters **29**, 385 (2017).
[26] Y. Hong-Gang, Y. Wang, X. Qing-Yang, X. Chang-Qing, J. Lightwave Technol. **24**, 1903 (2006).
[27] Y. Hong-Gang, Y. Wang, X. Chang-Qing, J. Wojcik, P. Mascher, IEEE J. Quantum Electron. **41**, 1492 (2005).
[28] F. Timofeey, G. Simin, M. Shatalv, S. Gurevich, P. Bayvel, R. Wyatt, I. Lealman, R. Kashyap, Fiber and Integrated Optics **19**, 327 (2000).
[29] J. Hashimoto, T. Takagi, T. Tato, G. Sasaki, M. Shigehara, K. Murashima, M. Shiozaki, T. Iwashima, IEEE J. Quantum Electron. **21**, 2002 (2003).
[30] M. M. K. Liu, Principle and Applications of Optical Communication, McGraw-Hill, USA, 1996.
[31] G. P. Agrawal, N. K. Dutta, Semiconductor Lasers, 2nd ed., Van Nostrand Reinhold, New York, 1993.
[32] H. Hisham, G. Mahdiraji, A. Abas, M. Mahdi, F. Mahamd Adikan, IEEE Photon. J. **4**, 1662 (2012).
[33] P. Krehlic, L. Sliwczynski, Opto-Electronics Review **12**, 187 (2004).

*Corresponding author: Husham_kadhum@yahoo.com